



ELSEVIER

Nuclear Physics B (Proc. Suppl.) 75B (1999) 124–128

NUCLEAR PHYSICS B  
PROCEEDINGS  
SUPPLEMENTS

# The latest results in charm physics of the experiment E687 at Fermilab

Gianluigi Boca for the E687 collaboration <sup>a</sup> \*<sup>a</sup>Dipartimento di Fisica Nucleare e Teorica and INFNvia Bassi 6  
27100 Pavia  
Italy

E687 has been a highly successful experiment on charm physics at Fermilab collecting approximately 100,000 fully reconstructed charm events. Still recently, after seven years since last data taking, E687 has produced world class physics results, the latest of which will be summarized in this article.

## 1. INTRODUCTION

The fixed target experiment E687 ran in 1990-91 at Fermilab with a  $\gamma$  beam of average energy  $\approx 220$  GeV on a 10% interaction length beryllium target ( $\approx 4$  cm). About 500,000,000 hadronic events were collected and 100,000 charm events reconstructed. With this statistics new results or confirmations were published in most of the charm physics areas (throughout this paper whenever a state is mentioned, the charge conjugate state is implied) : Cabibbo allowed, forbidden and double Cabibbo suppressed D, D<sub>s</sub> meson

\*Coauthors are : P. L. Frabetti, H. W. K. Cheung, J. P. Cumalat, C. Dallapiccola, J. F. Ginkel, W. E. Johns, M. S. Nehring, E. W. Vaandering, J. N. Butler, S. Cihangir, I. Gaines, P. H. Garbincius, L. Garren, S. A. Gourlay, D. J. Harding, P. Kasper, A. Kreymer, P. Lebrun, S. Shukla, M. Vittone, S. Bianco, F. L. Fabbrì, S. Sarwar, A. Zallo, C. Cawfield, R. Culbertson, R. W. Gardner, E. Gottschalk, R. Greene, K. Park, A. Rahimi, J. Wiss, G. Alimonti, G. Bellini, M. Boschini, D. Brambilla, B. Caccianiga, L. Cinquini, M. Di Corato, P. Dini, M. Giammarchi, P. Inzani, F. Leveraro, S. Malvezzi, D. Menasce, E. Meroni, L. Milazzo, L. Moroni, D. Pedrini, L. Perasso, F. Prelz, A. Sala, S. Sala, D. Torretta, D. Buchholz, D. Claes, B. Gobbi, B. O'Reilly, J. M. Bishop, N. M. Cason, C. J. Kennedy, G. N. Kim, T. F. Lin, D. L. Pusejlic, R. C. Ruchti, W. D. Shephard, J. A. Swiatek, Z. Y. Wu, V. Arena, G. Boca, G. Bonomi, C. Castoldi, G. Gianini, M. Merlo, S. P. Ratti, C. Riccardi, L. Viola, P. Vitulo, A. Lopez, L. Mendez, A. Mirles, E. Montiel, D. Olaya, E. Ramirez, C. Rivera, Y. Zhang, G. P. Grim, J.M. Link, V. S. Paolone, P. M. Yager, J. R. Wilson, J. Cao, M. Hosack, J. Hughes, P. D. Sheldon, F. Davenport, K. Cho, K. Danyo, T. Handler, B. G. Cheon, Y.S. Chung, J. S. Kang, K. Y. Kim, K.B. Lee, S.S. Myung

hadronic decays in 2, 3, 4 and 5 bodies; D, D<sub>s</sub> semileptonic decays, form factors and branching ratios; charm-anticharm production asymmetries and correlations; Dalitz analysis of  $D_s^+, D^+ \rightarrow K\pi^+\pi^-, K^+K^-\pi^+$  and  $\pi^+\pi^+\pi^-$ ;  $\Lambda_c^+, \Xi_c^+, \Xi_c^0, \Omega_c^0$  hadronic decays and branching ratios; lifetime measurements of all D mesons and singly charmed baryons; studies on the  $D^{**}, \Lambda_c^*, \Xi_c^*$  excited states; search for CP violation in  $D^+, D^0$  hadronic decays; search for  $D^+$  rare and forbidden decays and  $J/\Psi$  elastic photoproduction cross section.

In this paper I will describe the latest physics results published concerning a new  $\Xi_c^+$  lifetime and mass measurement, the evidence of a  $\Xi_c^*$  state and the Dalitz analysis of  $D_s^+, D^+ \rightarrow \pi^+\pi^+\pi^-$ .

The apparatus used in E687 is described in detail elsewhere<sup>[1]</sup> and it was a large aperture multiparticle spectrometer with good detection capabilities for charged hadrons and photons consisting of a 12 plane Si microstrip vertex detector, two analysis magnets, 5 multiwire proportional chambers, three multicell Čerenkov counters, two electromagnetic calorimeters (at small and wide angle), a hadron calorimeter, another electromagnetic calorimeter for measuring beam gamma energy, several muon counters and trigger scintillator hodoscopes.

## 2. $\Xi_c^+$ LIFETIME AND MASS MEASUREMENT

An improved measurement of the  $\Xi_c^+$  lifetime is important since it helps discriminating among

theoretical models incorporating string effects in singly charmed baryon decay (see ref.1 in [2]). In this measurement the channels  $\Xi_c^+ \rightarrow \Sigma^+ K^- \pi^+$  with : a)  $\Sigma^+ \rightarrow p\pi^0$  (channel never observed before) and b)  $\Sigma^+ \rightarrow n\pi^+$  were analysed in addition to the already existing<sup>[3]</sup> channel : c)  $\Xi_c^+ \rightarrow \Xi_c^- \pi^+ \pi^+$ . Details of the selection of the  $\Xi_c^+ \rightarrow \Sigma^+ K^- \pi^+$  channel can be found in [2]. The mass plot of the decay channels a), b) and c) and their sum are shown in figure 1. The invariant mass of the  $\Xi_c^+$  was fitted and a value of  $2465.8 \pm 1.9(stat.) \pm 2.5(syst.)$  MeV/c<sup>2</sup> was obtained after the study of systematics. For the life-

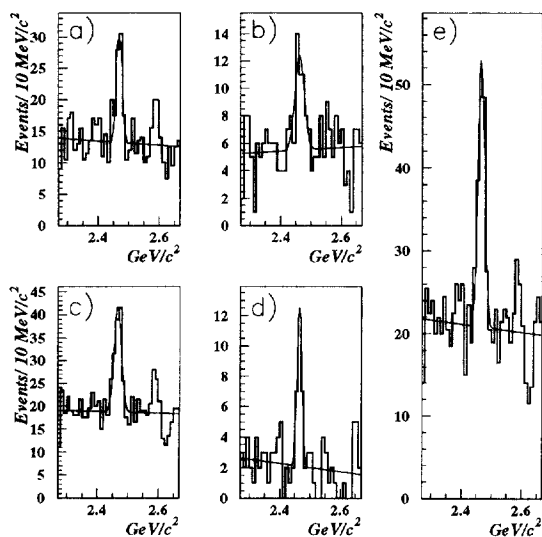


Figure 1. Invariant mass distribution for : a)  $\Xi_c^+ \rightarrow \Sigma^+(p\pi^0)K^- \pi^+$ ; b)  $\Xi_c^+ \rightarrow \Sigma^+(n\pi^+)K^- \pi^+$ ; c) sum of the two; d)  $\Xi_c^+ \rightarrow \Xi_c^- \pi^+ \pi^+$  e) sum of the three.

time measurement an isolation cut of  $l/\sigma_l > 3.8$  common to the three samples was used ( $l$  is the distance between the  $\Xi_c^+$  vertex and the primary vertex and  $\sigma_l$  is its error) while for the mass plots different  $l/\sigma_l$  cuts were used for different chan-

nels. The variable used in the lifetime fit was the reduced proper time :  $t' \equiv \frac{l - N\sigma_l}{\beta\gamma c}$  where  $N = 3.8$  and  $\beta\gamma$  is the Lorentz boost factor. Details of the fitting procedure and the likelihood function used for the total  $\Xi_c^+$  sample are described in [2]. For each channel the expected number of events  $n_i$  in the  $i^{th}$  reduced proper bin centered at  $t'_i$  is

$$n_i = S \frac{f(t'_i) e^{-\frac{t'_i}{\tau}}}{\sum_j f(t'_j) e^{-\frac{t'_j}{\tau}}} + B \frac{b_i}{\sum_j b_j}$$

the number of events as measured from the mass sidebands and  $f(t'_i)$  is the correction function estimated by a Montecarlo simulation,  $S$  are the signal events,  $B$  are the background events. The fitted lifetime was  $0.34^{+0.07}_{-0.05}(stat)$  ps. The studies of systematics indicated an error of 0.02 ps. The proper time distribution and the correction function are shown in figure 2. The  $\Xi_c^+$  yield is 56

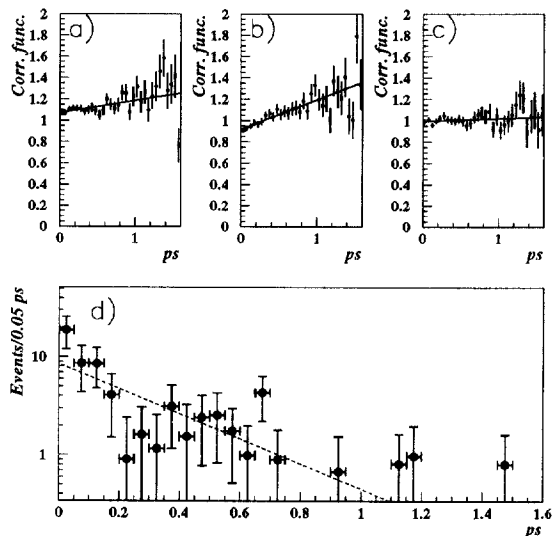


Figure 2. Correction functions for : a)  $\Xi_c^+ \rightarrow \Sigma^+(n\pi^+)K^- \pi^+$ ; b)  $\Xi_c^+ \rightarrow \Sigma^+(p\pi^0)K^- \pi^+$ ; c)  $\Xi_c^+ \rightarrow \Xi_c^- \pi^+ \pi^+$  d) Background subtracted, Montecarlo corrected reduced proper time distribution. The superimposed line is the result of the fit.

events. The E687 measurement is in good agreement and its error is comparable to the present PDG world average<sup>[4]</sup>.

### 3. EVIDENCE FOR A $\Xi^{*+} \rightarrow \Xi_c^0 \pi^+$ NARROW STATE

Excited baryon states provide a test on the predictions made by models based on QCD and lattice gauge calculations and rich information on the hadronic structure and on the forces governing that structure (see ref.1 in [5]). The lowest excited states of the  $\Xi_c$  baryon, in which the two light quarks are in a spin singlet, are expected to be two  $J^P = \frac{1}{2}^+$  states ( $\Xi'_c$ ). These states are believed to be below threshold for the decay to  $\Xi_c \pi$  and consequently to decay radiatively to  $\Xi_c \gamma$ . Recently they have been observed by WA89<sup>[6]</sup> and CLEO<sup>[7]</sup>. The next excited states ( $\Xi_c^*$ ) are expected to have  $J^P = \frac{3}{2}^+$  and to be above threshold for the  $\Xi_c \pi$  decay. The CLEO collaboration has reported<sup>[8]</sup> two mass differences:  $M(\Xi_c^+ \pi^-) - M(\Xi_c^+) = 178.2 \pm 0.5 \pm 1.0 \text{ MeV}/c^2$  and  $M(\Xi_c^0 \pi^+) - M(\Xi_c^0) = 174.3 \pm 0.5 \pm 1.0 \text{ MeV}/c^2$ . E687 has shown evidence of the  $\Xi_c^{*+}$  state decaying into  $\Xi_c^0 \pi^+$  and of the subsequent two new  $\Xi_c^0$  decays:  $\Xi_c^0 \rightarrow \Lambda K_s \pi^+ \pi^-$  and  $\Xi_c^0 \rightarrow \Lambda K^- \pi^+ \pi^+ \pi^-$ . Details of the analysis can be found in [5]. After a good  $\Xi_c^0$  candidate is found by the vertexing algorithm an additional  $\pi$  from the primary vertex is combined to form the  $\Xi_c^*$  state. Although no clear signal was observed in either the  $\Lambda K_s \pi^+ \pi^-$  or  $\Lambda K^- \pi^+ \pi^+ \pi^-$  invariant mass spectrum, due to the large combinatorial background, the scatter plot of  $\Delta M \equiv M(\Xi_c^0 \pi^+) - M(\Xi_c^0)$  versus the  $M(\Xi_c^0)$  shows a clear enhancement of events in the small box of fig. 3, whose boundaries are:  $|\Delta M - 177.1| < 4.0 \text{ MeV}/c^2$  and  $|M(\Xi_c^0) - 2470.3| < 24.0 \text{ MeV}/c^2$ . A two-dimensional gaussian fit of this signal gives  $S = 40.7 \pm 8.2$  signal events with  $\frac{S}{\sqrt{B}} = 6.7$  statistical significance. Selecting events within the two horizontal lines that satisfy the cut  $|M(\Xi_c^0) - 2470.3| < 24.0 \text{ MeV}/c^2$  one obtains the  $\Delta M$  distribution shown in fig. 3b. A fit and the study of systematics gives the value of  $\Delta M = 177.1 \pm 0.5 \pm 1.1 \text{ MeV}/c^2$ . Similarly, selecting events between the vertical lines corresponding to the  $\Delta M$  cut one obtains the invariant

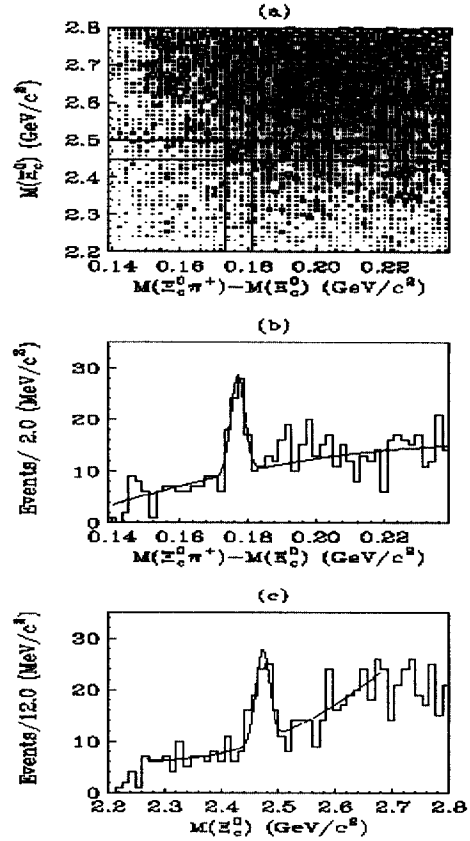


Figure 3. a)  $\Delta M$  versus  $M(\Xi_c^0)$  scatter plot for the  $\Xi_c^0 \rightarrow \Lambda K_s \pi^+ \pi^-$  and  $\Xi_c^0 \rightarrow \Lambda K^- \pi^+ \pi^+ \pi^-$  combined sample; b)  $\Delta M$  distribution c)  $M(\Xi_c^0)$  distribution.

mass distribution of fig. 3c. The result of a fit and study of systematics is  $M(\Xi_c^0) = 2471.8 \pm 3.6 \pm 3.0 \text{ MeV}/c^2$ . The yield calculated from the plot in fig. 3b and 3c agree well with the one of the two-dimensional scatter plot. This leads to believe that these events originate from a higher mass state ( $\Xi_c^{*+}$ ) decaying into  $\Xi_c^0 \pi^+$ . This is confirmed also by the scatter plot of the wrong sign  $\Delta M \equiv M(\Xi_c^0 \pi^-) - M(\Xi_c^0)$  versus  $M(\Xi_c^0)$  (not shown here) where no signal is observed. Separating the contribution of the two decay channels in the scatter plot of fig. 3a one obtains fig. 4a,b and 4c,d for the  $\Xi_c^0 \rightarrow \Lambda K^- \pi^+ \pi^+ \pi^-$

and  $\Xi_c^0 \rightarrow \Lambda K_s \pi^+ \pi^-$  channels respectively. Fits

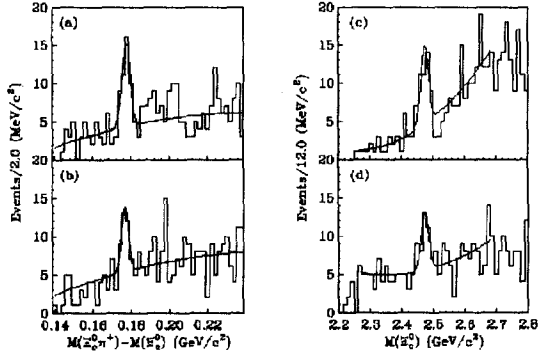


Figure 4. The mass difference distributions and the  $\Xi_c^0$  invariant mass distribution for : a) and c) the  $\Xi_c^0 \rightarrow \Lambda K^- \pi^+ \pi^+ \pi^-$  decay; b) and d) the  $\Xi_c^0 \rightarrow \Lambda K_s \pi^+ \pi^-$  decay.

to Gaussian signal plus polynomial background yields  $26.5 \pm 8.0$  and  $19.8 \pm 7.8$  events for the two channels, in agreement with the yield quoted above for the total sample. Also the  $\Delta M$  and  $M(\Xi_c^0)$  values are in agreement with the ones obtained with the total sample.

#### 4. ANALYSIS OF THE $D^+$ , $D_s^+ \rightarrow \pi^+ \pi^+ \pi^-$ DALITZ PLOTS

The amplitude analysis of non-leptonic decays is an excellent tool for studying charmed hadron dynamics. In particular the  $D_s^+ \rightarrow \pi^+ \pi^+ \pi^-$  decay is Cabibbo allowed and can provide crucial information on the dynamics of the decay. In E687 it was possible to select a sample of  $D^+$  and  $D_s^+$  decaying into three pions using a 'candidate driven' algorithm<sup>[9]</sup>. All the details on this analysis can be found in [10]. The three pion invariant mass of the selected sample is shown in fig. 5.a; in fig. 5.b the additional requirement that the  $D$  vertex lie outside the target is imposed. For the Dalitz analysis the much cleaner sample of fig. 5.b is used. This mass plot is fitted using two Gaussians for the  $D^+$  and  $D_s^+$  signals, a

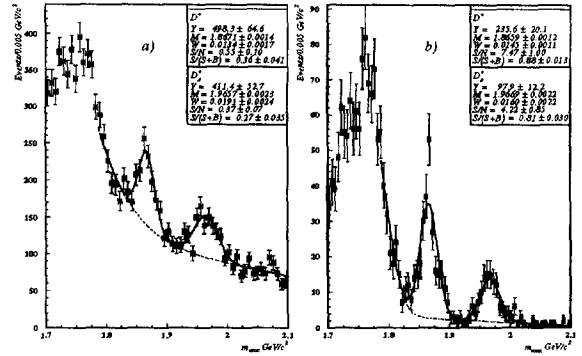


Figure 5. The  $\pi^+ \pi^+ \pi^-$  mass distributions : a) 'candidate driven' sample; b) 'candidate driven' and out of target sample

Gaussian shape for the  $K \pi \pi$  reflection tail at high masses and a second order polynomial for the remaining background. The yield was  $235.6 \pm 20.1$  and  $97.9 \pm 12.2$  events for the  $D^+$  and  $D_s^+$  signal respectively. It would be too long here to summarize all the details of the Dalitz analysis formalism and the resonances used in the fit; these can be found in [10]. Only the final results are shown in table 1 for the  $D_s^+ \rightarrow \pi^+ \pi^+ \pi^-$  and in table 2 for the  $D^+ \rightarrow \pi^+ \pi^+ \pi^-$  channel. From table 1 it is clear that the  $D_s^+$  decay is mainly a two-body process since only the  $f_2(1270)$ ,  $f_0(980)$  and the  $S(1475)$  resonances have non-zero amplitude coefficients exceeding  $3\sigma$  significance. The  $S(1475)$  is a state parametrized with a Breit-Wigner with mass and width fitted on the Dalitz plot itself (this was done because of the present major experimental uncertainty about dipion scalar resonances in the  $\pi^+ \pi^-$  mass region around 1500  $\text{MeV}/c^2$ ). The fitted parameters are remarkably consistent with the  $f_0(1500)$  entry of the PDG<sup>[4]</sup>. The consistency with zero of the  $\rho$  and Non Resonant contribution may be interpreted with the absence of the annihilation diagram in the  $D_s^+$  decay. As opposite to the  $D_s^+$  case, from table 2 one sees that the  $D^+$  decay is mainly in the Non-Resonant state with a smaller contribution from

Table 1

 $D_s^+ \rightarrow \pi^+\pi^+\pi^-$  results

Decay mode	Decay fraction	Phase (degrees)	Amplitude coefficient
Non Res.	$0.121 \pm 0.115 \pm 0.044$	$235 \pm 22 \pm 2$	$0.34 \pm 0.14$
$\rho(770)\pi$	$0.023 \pm 0.027 \pm 0.011$	$53 \pm 44 \pm 10$	$0.15 \pm 0.09$
$f_2(1270)\pi$	$0.123 \pm 0.056 \pm 0.018$	$100 \pm 18 \pm 6$	$0.34 \pm 0.09$
$f_0(980)\pi$	$1.074 \pm 0.140 \pm 0.043$	0( <i>fixed</i> )	1( <i>fixed</i> )
$S(1475)\pi$	$0.274 \pm 0.114 \pm 0.019$	$234 \pm 15 \pm 4$	$0.50 \pm 0.13$

Table 2

 $D^+ \rightarrow \pi^+\pi^+\pi^-$  results

Decay mode	Decay fraction	Phase (degrees)	Amplitude coefficient
Non Res.	$0.589 \pm 0.105 \pm 0.081$	0( <i>fixed</i> )	1( <i>fixed</i> )
$\rho(770)\pi$	$0.289 \pm 0.055 \pm 0.058$	$27 \pm 14 \pm 11$	$0.70 \pm 0.11$
$f_2(1270)\pi$	$0.052 \pm 0.034 \pm 0.035$	$207 \pm 17 \pm 4$	$0.30 \pm 0.11$
$f_0(980)\pi$	$0.027 \pm 0.031 \pm 0.038$	$197 \pm 28 \pm 24$	$0.22 \pm 0.13$

Table 3

Branching ratio measurement

	$\frac{\Gamma(D^+ \rightarrow \pi^+\pi^+\pi^-)}{\Gamma(D^+ \rightarrow K^-\pi^+\pi^+)}$
E687	$.043 \pm .003 \pm .003$
E691	$.035 \pm .007 \pm .003$
WA82	$.032 \pm .011 \pm .003$
MarkIII	$.042 \pm .016 \pm .010$
	$\frac{\Gamma(D^+ \rightarrow \pi^+\pi^+\pi^-)}{\Gamma(D^+ \rightarrow \phi\pi^+)}$
E687	$.328 \pm .058 \pm .058$
E691	$.44 \pm .10 \pm .04$
WA82	$.33 \pm .10 \pm .04$
	$\frac{\Gamma(D^+ \rightarrow \pi^+\pi^+\pi^-)}{\Gamma(D^+ \rightarrow K^-K^+\pi^+)}$
E687	$.265 \pm .041 \pm .031$

the two-body channel with the  $\rho(770)$  resonance. Finally in table 3, three relative branching ratios are shown together with a comparison with different experiments. One can conclude that E687 results are in reasonable agreement with the previous determinations and significantly increase the precision of the measurements.

## REFERENCES

1. P.L.Frabetti et al., Nucl. Instrum. Methods A

320 (1992).

2. P.L.Frabetti et al., Phys.Lett., B427 (1998) 211.
3. P.L.Frabetti et al., Phys. Rev. Lett. 70 (1993) 1381.
4. Review of Particle Physics, The European Physical Journal C (1998).
5. P.L.Frabetti et al., Phys. Lett. B426 (1998) 403.
6. R.Werding et al., Proceedings of the 27<sup>th</sup> International Conference on High Energy Physics (1995) 1023.
7. T.E.Coan et al., CLEO Conf. 97-29 and EPS 97-393 (1997)
8. P.Avery et al., Phys. Rev. Lett. 75 (1995) 4364  
L.Gibbons et al., Phys. Rev. Lett. 77 (1996) 810.
9. P.L.Frabetti et al., Nucl. Instrum. Methods A 320 (1992) 519;  
P.L.Frabetti et al., Nucl. Instrum. Methods A 329 (1993) 62;  
P.L.Frabetti et al., Phys. Lett. B331 (1994) 217; P.L.Frabetti et al., Phys. Lett. B351 (1995) 591;
10. P.L.Frabetti et al., Phys. Lett. B407 (1997) 79.